Successful treatment of a novel type I interferonopathy due to a *de novo PSMB9* gene mutation with a Janus kinase inhibitor

Shinsuke Kataoka, MD[1†], Nozomu Kawashima, MD, PhD[1†], Yusuke Okuno, MD, PhD[2], Hideki Muramatsu, MD, PhD[1], Shunsuke Miwata, MD[1], Kotaro Narita, MD[1], Motoharu Hamada, MD, PhD[1], Norihiro Murakami, MD, PhD[1], Rieko Taniguchi, MD, PhD[1], Daisuke Ichikawa, MD[1], Hironobu Kitazawa, MD[1], Kyogo Suzuki, MD, PhD[1], Eri Nishikawa, MD, PhD[1], Atsushi Narita, MD, PhD[1], Nobuhiro Nishio, MD, PhD[1,3], Hidenori Yamamoto, MD[1], Yoshie Fukasawa, MD[1], Taichi Kato, MD, PhD[1], Hiroyuki Yamamoto, MD, PhD[1], Jun Natsume, MD, PhD[1], Seiji Kojima, MD, PhD[1], Ichizo Nishino, MD, PhD[4], Takeshi Taketani, MD, PhD[5], Hidenori Ohnishi, MD, PhD[6], and Yoshiyuki Takahashi, MD, PhD[1]

[1]Department of Pediatrics, Nagoya University Graduate School of Medicine, Nagoya, Japan

[2]Medical Genomics Center, Nagoya University Hospital, Nagoya, Japan

[3]Center for Advanced Medicine and Clinical Research, Nagoya University Hospital, Nagoya, Japan

[4]Department of Neuromuscular Research, National Institute of Neuroscience, National Center of Neurology and Psychiatry, Tokyo, Japan

[5]Department of Pediatrics, Shimane University Faculty of Medicine, Shimane, Japan

[6]Department of Pediatrics, Gifu University Graduate School of Medicine, Gifu, Japan

† These authors contributed equally to this work.

Corresponding author

Yoshiyuki Takahashi, MD, PhD. Professor, Department of Pediatrics,

Nagoya University Graduate School of Medicine,

65 Tsurumai-cho, Showa-ku, Nagoya, Aichi, 466-8550 Japan

Phone: +81-52-744-2294 FAX: +81-52-744-2974

E-mail: ytakaha@med.nagoya-u.ac.jp

Funding

This work was supported by “Research on Measures for Intractable diseases” Project from the Ministry of Health, Labour and Welfare of Japan, and partly by Intramural Research Grant for Neurological and Psychiatric Disorders of National Center of Neurology and Psychiatry.

Conflict of Interest

The authors declare that they have no relevant conflicts of interest.

Abstract

Background: Type I interferonopathies are a recently established subgroup of autoinflammatory diseases caused by mutations in genes associated with proteasome degradation or cytoplasmic RNA and DNA sensing pathways.

Objective: This study aimed to unveil the molecular pathogenesis of a patient with novel type I interferonopathy, for which no known genetic mutations have been identified.

Methods: We performed the whole exome sequencing (WES) of a 1-month-old boy with novel type I interferonopathy. We also investigated proteasome activities using patient-derived B lymphoblastoid cell lines (LCLs) and normal LCLs transduced with the mutant gene.

Results: WES identified a *de novo* proteasome 20S subunit beta 9 (*PSMB9*) p.G156D mutation in the patient who developed fever, a chilblain-like skin rash, myositis, and severe pulmonary hypertension due to the hyperactivation of interferon-alpha. Patient-derived LCLs revealed reduced proteasome activities, and exogenous transduction of mutant *PSMB9* p.G156D into normal LCLs significantly suppressed proteasome activities, and the endogenous PSMB9 protein was lost along with the reduction of other immunoproteasome subunits, PSMB8 and PSMB10 proteins. He responded to the administration of a Janus kinase (JAK) inhibitor, tofacitinib, and he was successfully withdrawn from veno-arterial extracorporeal membranous

oxygenation. At 7 months of age, he received an unrelated cord blood transplantation. At 2 years post transplantation, he no longer required tofacitinib and experienced no disease recurrence.

Conclusion: We present the case of a patient with a novel type I interferonopathy caused by a *de novo PSMB9* p.G156D mutation which suppressed the wild-type PSMB9 protein expression. JAK inhibitor and stem cell transplantation could be curative therapies in patients with severe interferonopathies.

Clinical Implications: A *de novo PSMB9* mutation causes novel type I interferonopathy. The use of a JAK inhibitor along with stem cell transplantation may treat the severe form of type I interferonopathies.

Capsule Summary

We report a novel type I interferonopathy caused by a *de novo* missense mutation of the *PSMB9* gene. Treatment with a JAK inhibitor, tofacitinib, resulted in resolution of symptoms, including severe pulmonary hypertension.

Key words

JAK inhibitor, interferonopathy, pulmonary hypertension, proteasome subunit beta type 9 (*PSMB9*)

Abbreviations

Aicardi–Goutières syndrome (AGS), STING-associated vasculopathy with onset in infancy (SAVI), chronic atypical neutrophilic dermatosis with lipodystrophy and elevated temperature (CANDLE), Janus kinase (JAK), proteasome 20S subunit beta 9 (*PSMB9*), creatine phosphokinase (CPK), computed tomography (CT), interferon α (IFN-α), nitric oxide (NO), Veno-arterial extracorporeal membranous oxygenation (VA-ECMO), graft versus host disease (GVHD), lymphoblastoid cell lines (LCLs), immunoblot (IB), wild-type (WT)

Introduction

Autoinflammatory diseases are characterized by dysregulation of innate immunity and systemic inflammation in the absence of antigen-specific T cells or high-titer autoantibodies[1].

Type I interferonopathies are a recently established subgroup of autoinflammatory disease that includes Aicardi–Goutières syndrome (AGS), STING-associated vasculopathy with onset in infancy (SAVI), and chronic atypical neutrophilic dermatosis with lipodystrophy and elevated temperature (CANDLE) syndrome. Patients with type I interferonopathy shared a several clinical characteristics, including bilateral calcifications of the basal ganglia, chilblain-like rashes, and liver dysfunction[2]. Each subtype includes disease-specific severe complications, such as early-onset encephalopathy associated with AGS[3] and pulmonary hypertension observed in patients diagnosed with SAVI[4].

The common pathogenic mechanism shared by all of these diseases is overactivation of the type I interferon pathway caused by mutations in genes associated with proteasome degradation or cytoplasmic RNA and DNA sensing pathways[2]. *In vitro* experiments using patient-derived primary cells[4] and anecdotal case reports have suggested that Janus kinase (JAK) inhibitors, including tofacitinib[5] and ruxolutinib[6], may be effective for the treatment of these disorders. Here, we report the case of a novel type I interferonopathy in a patient with a

de novo proteasome 20S subunit beta 9 (*PSMB9*) mutation who was successfully treated with tofacitinib as a bridging therapy prior to allogeneic stem cell transplantation.

Methods

For detailed methods, please see the Methods section in this article's Online Repository at www.jacionline.org.

Results and Discussion

A 1-month-old boy visited a hospital for evaluation and treatment of skin rashes, fever, pale face due to respiratory failure, and cluster seizures. Initial blood tests revealed pancytopenia (white blood cell count at 3.83×10^9/L, hemoglobin at 7.6 g/dL, and platelets at 52×10^9/L), elevated levels of liver enzymes (aspartate aminotransferase at 923 IU/L, alanine aminotransferase at 426 IU/L), marked elevation of creatine phosphokinase (CPK at 26,839 IU/L), and abnormal coagulation tests, including prothrombin time-international normalized ratio at 1.40 sec, fibrinogen at 105 mg/dL, fibrin degradation products at 29.8 mg/L, D-dimers at 21.0 mg/L, and antithrombin at 33 %. Cerebrospinal fluid tests were notable for increased levels of total protein (148.2 mg/dL), normal glucose (45 mg/dL), and a normal cell count (11

$\times 10^6$/L). Acute encephalopathy was suspected; the patient was initially treated with acyclovir, cefotaxime, intravenous immunoglobulin, and methylprednisolone pulse therapy. His symptoms improved temporarily, but fever, elevation of CPK, and seizures reappeared rapidly.

Serologic screening for infectious pathogens and various encephalopathy-associated autoantibodies were uniformly negative. Although serum PCR tests for BK virus and JC virus were transiently positive after methylprednisolone pulse therapy, we confirmed that viremia test had negative outcomes without any specific antiviral treatment before hematopoietic stem cell transplantation. The lymphocyte subset analysis (CD3, CD4, CD8, and CD19 cell counts) revealed mild lymphocytopenia, while the lymphocyte stimulation tests with phytohemagglutinin and concanavalin A were within the normal limits (Table E1 in the Online Repository at www.jacionline.org). Head computed tomography (CT) revealed bilateral calcification of the basal ganglia (Fig 1, *A*), which led to the suspicion of a type I interferonopathy. Although we could not eliminate the possibility of the effect of viral infection, elevated levels of interferon α (IFN-α) were detected in both serum (36.5 pg/mL) and spinal fluid (6.9 pg/mL) (Fig 1, *E*). A biopsy of the left quadriceps revealed primarily immature muscle fibers that were round and small, measuring 7–16 microns in diameter. Immuno-histochemical staining confirmed the expression of HLA class I molecule and deposition of the

membrane attack complex on myofibrotic membranes; these results suggested immune-mediated damage to the muscle tissue (Fig 1, *B*).

Chest CT scan revealed mild pulmonary infiltrative shadows bilaterally in the dorsal lung fields and mild cardiomegaly, and an echocardiogram revealed severe pulmonary hypertension with tricuspid regurgitation at a peak velocity of 5.18 m/sec; the estimated pressure gradient between the right ventricle and right atrium at peak systole was 107 mmHg (Fig 1, *C* and videos E1 and E2). The pulmonary hypertension was unresponsive to multiple lines of treatment, including epoprostenol sodium, sildenafil citrate, milrinone, macitentan, and inhalation of nitric oxide (NO). Veno-arterial extracorporeal membranous oxygenation (VA-ECMO) was introduced due to progression of right heart failure.

Under the approval from the institutional review board, we initiated therapy with the JAK inhibitor, tofacitinib, at a dose of 0.2 mg/kg/day twice daily on day 1 after the VA-ECMO induction; the dose was increased to 0.3 mg/kg/day after 2 weeks. Shortly after starting on tofacitinib, the serum level of CPK normalized and chilblain-like rashes improved. VA-ECMO and NO inhalation were successfully withdrawn after 16 days and 39 days, respectively, without further complications. His pulmonary hypertension was well-controlled on sildenafil citrate and macitentan.

At 7 months of age, he underwent an HLA 7/8 allele-matched unrelated cord blood transplantation after a reduced intensity conditioning regimen that included fludarabine (120 mg/m^2) and melphalan (140 mg/m^2) with total body irradiation at 3 Gy. Tacrolimus and short-term methotrexate were used as prophylaxis against graft versus host disease (GVHD). He was engrafted at day 14 after transplantation; he developed mild skin GVHD which improved without additional treatment. He also developed post-transplant nephrotic syndrome at day 104 which responded well to steroids and cyclosporin A. Hematopoiesis was evaluated with short tandem repeat analysis that revealed stable mixed donor chimerism undergoing gradual increase, determined at 38.1% on day 28, 47.1% on day 116, 61.7% on day 179, 67.5% on day 350, and 63.1% on day 645.

At 2 years post transplantation, the patient no longer requires tofacitinib or vasodilator drugs and is in good health without fever, skin rash, pulmonary hypertension, or other symptoms associated with type I interferonopathy.

Whole exome sequencing analysis identified a *de novo* heterozygous missense variant of *PSMB9* (NM_002800.5:c. 467G>A, p.G156D) in our patient/proband, which has not been previously reported as a causative gene for human disease (Fig 1, *D*), and we confirmed that his parents had only wild-type alleles in *PSMB9*. Three-dimensional structure analysis

revealed that the PSMB9 substitution sites were adjacent to one another in the two beta-rings of the immunoproteasome (Fig 1, *F* and *G* and *H* and *I*). No other pathogenic variants associated with any known inherited diseases including autoinflammatory diseases were detected.

A proteasome activity assay revealed that proband-derived lymphoblastoid cell lines (LCLs) (Y375 cells) that included the heterozygous *PSMB9* mutation had lost most of the chymotrypsin-like, trypsin-like, and caspase-like protease activities; by contrast, the LCLs derived from the father (A151) and mother (A139) that both maintained wild-type *PSMB9* alleles have activity that was comparable to that detected in LCLs derived from three unrelated healthy volunteers (Fig 2, *A* and *B*). The proteasome inhibitor, epoxomicin, completely suppressed protease activities detected in all LCLs. We also confirmed that IFN-α in cultured media was significantly elevated in proband-derived LCLs (Y375) when compared to healthy control cells (A151 and A139) (Fig 2, *C*).

We established A151 cells with lentivirus-mediated overexpression of FLAG-tagged mutant PSMB9 (A151_EGFP_PSMB9^{G156D}) and FLAG-tagged wild-type (WT) PSMB9 (A151_ EGFP_PSMB9^{WT}); A151 cells transduced with empty vector (A151_EGFP) served as a control. Exogenous expression was confirmed via bicistronic expression of EGFP (data not

shown). Similar levels of proteasome activity were detected in the primary A151 cells, the A151_EGFP_PSMB9^{WT} cells, and A151_EGFP cells. By contrast, the A151_EGFP_PSMB9^{G156D} cells had significantly lower proteasome activity; these results suggested that this mutation suppressed protease activity via a dominant negative mechanism (Fig 2, *B*).

Immunoblot (IB) with polyclonal and monoclonal anti-PSMB9 antibodies uncovered a 10kDa larger protein band in lysates from the proband-derived LCLs (Y375) compared to bands identified in LCLs from the father (A151) and mother (A139) (Fig 2, *D*), which led us to hypothesize that the larger protein band is a ubiquitinated PSMB9 protein. The level of total ubiquitin-coupled proteins remained constant when comparing Y375 to those of A151 and A139. IB using an anti-ubiquitin antibody to co-precipitate proteins detected with the anti-PSMB9 antibody revealed enhanced ubiquitination in Y375 compared with A151 and A139 (Fig 2, *E*). These results suggested enhanced ubiquitination of the PSMB9 protein in the proband cells which served to promote its degradation.

IB with the anti-FLAG antibody confirmed exogenous expression of PSMB9^{WT} protein in A151_EGFP_PSMB9^{WT} cells; by contrast, no exogenous PSMB9^{G156D} expression was detected in A151_EGFP_PSMB9^{G156D} cells (Fig 2, *D*). Furthermore, IB using anti-PSMB9

antibody revealed decreased levels of endogenous $PSMB9^{WT}$ protein expression in A151_EGFP_$PSMB9^{G156D}$ cells compared to A151_EGFP_$PSMB9^{WT}$ cells and A151_EGFP cells. IB for other subunits of immunoproteasome with anti-PSMB8 and anti-PSMB10 antibodies revealed that both PSMB8 and PSMB10 were downregulated in proband-derived LCLs (Y375) and father-derived LCLs with mutant PSMB9 G156D (A151_EGFP_$PSMB9^{G156D}$) (Fig E1). These results suggest that the mechanism by which mutant PSMB9 p.G156D protein impairs immunoproteasome function is due to the isolated role of PSMB9 and its impact on other elements of the immunoproteasome, such as PSMB8 and PSMB10. However, whether other PSMB9 amino acid substitution mutations could have similar or different physiological effects needs to be clarified in the future studies.

To investigate the relationship between IFN-α elevation and the JAK-STAT1 pathway in his disease, we evaluated the phosphorylation of STAT1 in LCLs. We found that endogenous STAT1 was constitutively phosphorylated in both proband-derived LCLs (Y375) and healthy control LCLs (A151 and A139), although the phosphorylation was weak (Fig E2). Therefore, we next measured the phosphorylation levels of STAT1 in the presence of exogenous IFN-α. The phosphorylation levels of STAT1 in healthy control (A151) decreased to the basal levels after 8 h of IFN-α stimulation, whereas Y375 maintained high

phosphorylation levels even 24 h after the IFN-α stimulation. Furthermore, we confirmed that this exogenous IFN-α induced STAT1 phosphorylation in Y375 was inhibited by the addition of the JAK inhibitor tofacitinib (Fig 2, *F*).

Taken together, these results suggested that mutant PSMB9 p.G156D protein had a dominant negative effect via its capacity to promote degradation and to inhibit the function of normal PSMB9 protein. CANDLE syndrome, a typical type I interferonopathy, is caused by a biallelic loss-of-function mutation in the *PSMB8* gene[7]. *PSMB9* and *PSMB8* encode the catalytic subunits of the immunoproteasomes beta-1i and beta-5i, respectively. The *PSMB9* p.G156D mutation is a new proteasome-associated autoinflammatory syndrome with symptoms and molecular mechanisms that are similar to those described previously.

In vitro experiments using patient-derived primary cells[4] together with anecdotal case reports suggested that JAK inhibitors, such as tofacitinib[5] and ruxolutinib[6], may be promising drugs to be used to treat type I interferonopathies. In our patient case, administration of tofacitinib resulted in complete resolution of clinical symptoms, including normalization of life-threatening pulmonary hypertension and elevated serum levels of CPK. Following bridging therapy with the JAK inhibitor, our patient underwent cord blood transplantation and achieved long-term survival; we were able to discontinue tofacitinib without flare-ups of

symptoms associated with interferonopathy.

In conclusion, we present here the case of a patient with a novel type I interferonopathy caused by a *de novo PSMB9* p.G156D mutation with dominant negative effect. He was successfully treated with tofacitinib followed by allogeneic cord blood stem cell transplantation. These results suggest the use of JAK inhibitor and stem cell transplantation as curative therapies in patients with severe interferonopathies.

Acknowledgments

We thank the patient and his family members for cooperatively providing samples. We thank Ms. Yoshie Miura and Dr. Yasutomo Itoh for their professional technical assistance and Dr. Emi Kadoi and Dr. Kunihiro Shinoda for providing clinical data on viral infections and antibodies.

Author Contributions

S.K. and N.K. performed research and wrote the paper. Y.O. and H. M. designed and performed the research, led the project and wrote the paper. S.K., K.N., M.H., N.M., R.T., D.I., H.K., K.S., E.N., A.N., N.N., H.Y., Y.F., T.K., H.Y., and J.N. collected clinical sample and data. I.N. performed pathological diagnosis. T.T. performed viral analysis. S.K., H.O., and Y.T.

designed the research and analyzed data. All authors critically reviewed the content of the manuscript and agreed on the final version of the manuscript.

References

1. McDermott MF, Aksentijevich I, Galon J, McDermott EM, William Ogunkolade B, Centola M, et al. Germline mutations in the extracellular domains of the 55 kDa TNF receptor, TNFR1, define a family of dominantly inherited autoinflammatory syndromes. Cell. 1999;97:133–144.

2. Kim H, Sanchez GAM, Goldbach-Mansky R. Insights from Mendelian interferonopathies: comparison of CANDLE, SAVI with AGS, monogenic lupus. J Mol Med. 2016;94:1111–1127.

3. Rice G, Patrick T, Parmar R, Taylor CF, Aeby A, Aicardi J, et al. Clinical and molecular phenotype of Aicardi-Goutières syndrome. Am J Hum Genet. 2007;81:713–725.

4. Liu Y, Jesus AA, Marrero B, Yang D, Ramsey SE, Montealegre Sanchez GA, et al. Activated STING in a vascular and pulmonary syndrome. N Engl J Med. 2014;371:507–518.

5. Seo J, Kang JA, Suh DI, Park EB, Lee CR, Choi SA, et al. Tofacitinib relieves symptoms of stimulator of interferon genes (STING)–associated vasculopathy with onset in infancy caused by 2 de novo variants in TMEM173. J Allergy Clin Immunol. 2017;139:1396–1399.

6. Frémond ML, Rodero MP, Jeremiah N, Belot A, Jeziorski E, Duffy D, et al. Efficacy of the Janus kinase 1/2 inhibitor ruxolitinib in the treatment of vasculopathy associated with TMEM173-activating mutations in 3 children. J Allergy Clin Immunol. 2016;138:1752–1755.

7. Liu Y, Ramot Y, Torrelo A, Paller AS, Si N, Babay S, et al. Mutations in proteasome subunit β type 8 cause chronic atypical neutrophilic dermatosis with lipodystrophy and elevated temperature with evidence of genetic and phenotypic heterogeneity. Arthritis Rheum. 2012;64:895–907.

Figure Legends

Fig 1. Clinical presentations and *in silico* modeling of mutated PSMB9 protein

(A) Head computed tomography (CT), *yellow arrowheads* indicate calcifications of basal

ganglia. (B) Biopsy specimen from the quadriceps femoris muscle; *yellow circle* indicates a muscle fiber with the aberrant small and round shape. (C) Echocardiogram documenting pulmonary hypertension; 4 chamber view with color Doppler prior to the initiation of tofacitinib and VA-ECMO. (D) Sanger sequencing; a *de novo* heterozygous c.467G>A (p.G156D) mutation was identified in proband. (E) Transition of IFN-α and CRP value; the black line and the gray line indicate the transitions of the IFN-α value and the CRP value, respectively. Tofacitinib was initiated on day 37 after interferonopathy diagnosis at a dose of 0.2 mg/kg/day twice daily; the dose was increased to 0.3 mg/kg/day after 2 weeks. (F) Three-dimensional structure of PSMB9; the impact of the *PSMB9* mutation was modeled based on the Cryo-electron microscopy structure of the human immunoproteasome (PDB entry code: 6AVO). Blue and green ribbons show PSMB9 protein on two separate β-rings. (G and H and I) Close-up views show three patterns where the two PSMB9 proteins are wild-type or mutant type. The positions of the mutant amino acid are shown in orange for the wild-type (G156) and red for the mutant type (D156), respectively.

Fig 2. Functional analysis of *PSMB9* G156D mutation

(A) Proteasome activity in proband-derived LCLs (Y375). Black bar, white bar, and gray bar

indicate chymotrypsin-like, trypsin-like, and caspase-like activities, respectively. The addition of epoxomicin results in the suppression of the proteasome activities in control LCLs established from three healthy volunteers. (B) The proteasome activity in LCLs from the proband (Y375), mother (A139), father (A151), A151 transduced with mutant *PSMB9* (A151_EGFP_PSMB9^{G156D}), with WT *PSMB9* (A151_EGFP_PSMB9^{WT}), and with the empty vector (A151_EGFP). (C) The IFN-α levels in LCLs cultured media after 24-h and 48-h culture. The black, white, and gray bars indicate proband-derived LCLs, father-derived LCLs, and mother-derived LCLs, respectively. (D) Immunoblot probed with polyclonal and monoclonal anti-PSMB9, anti-FLAG, and anti-GFP antibodies. (E) Immunoprecipitation with monoclonal anti-PSMB9; anti-ubiquitin and monoclonal anti-PSMB9 antibodies were used for IB. (F) Immunoblot probed with anti-phosphorylated STAT1 (Tyr 701) and anti-STAT1 antibodies in proband-derived and father-derived LCLs after exogenous IFN-α stimulation without and with tofacitinib.

FIG 1

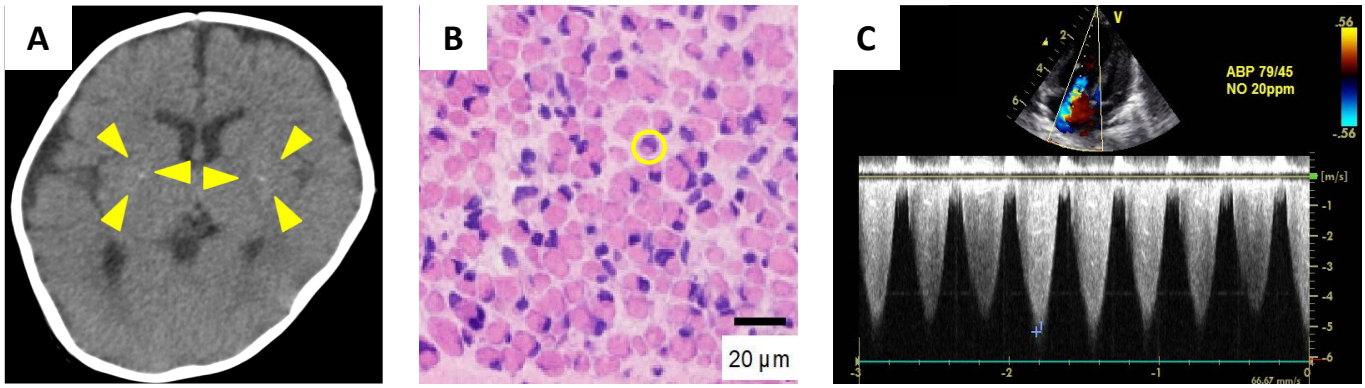

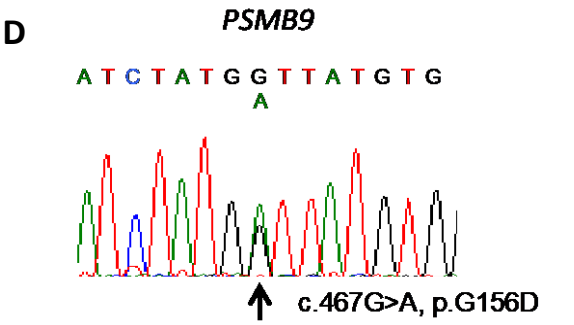

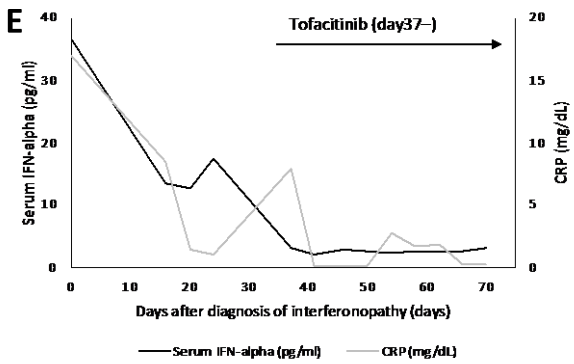

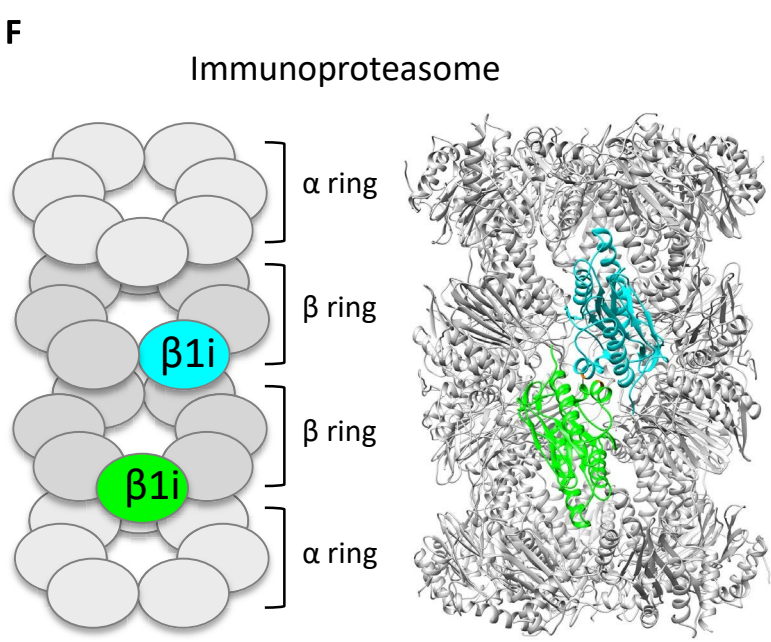

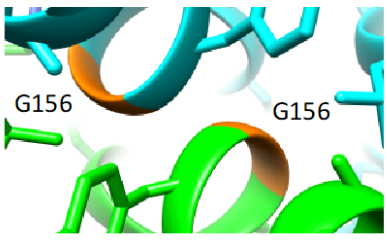

PSMB9 WT / PSMB9 WT

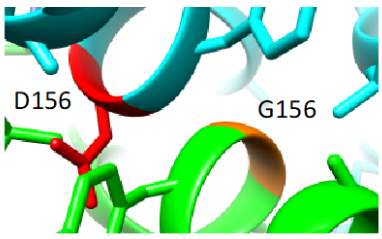

PSMB9 G156D / PSMB9 WT

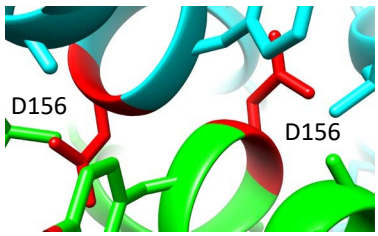

PSMB9 G156D / PSMB9 G156D

FIG 2

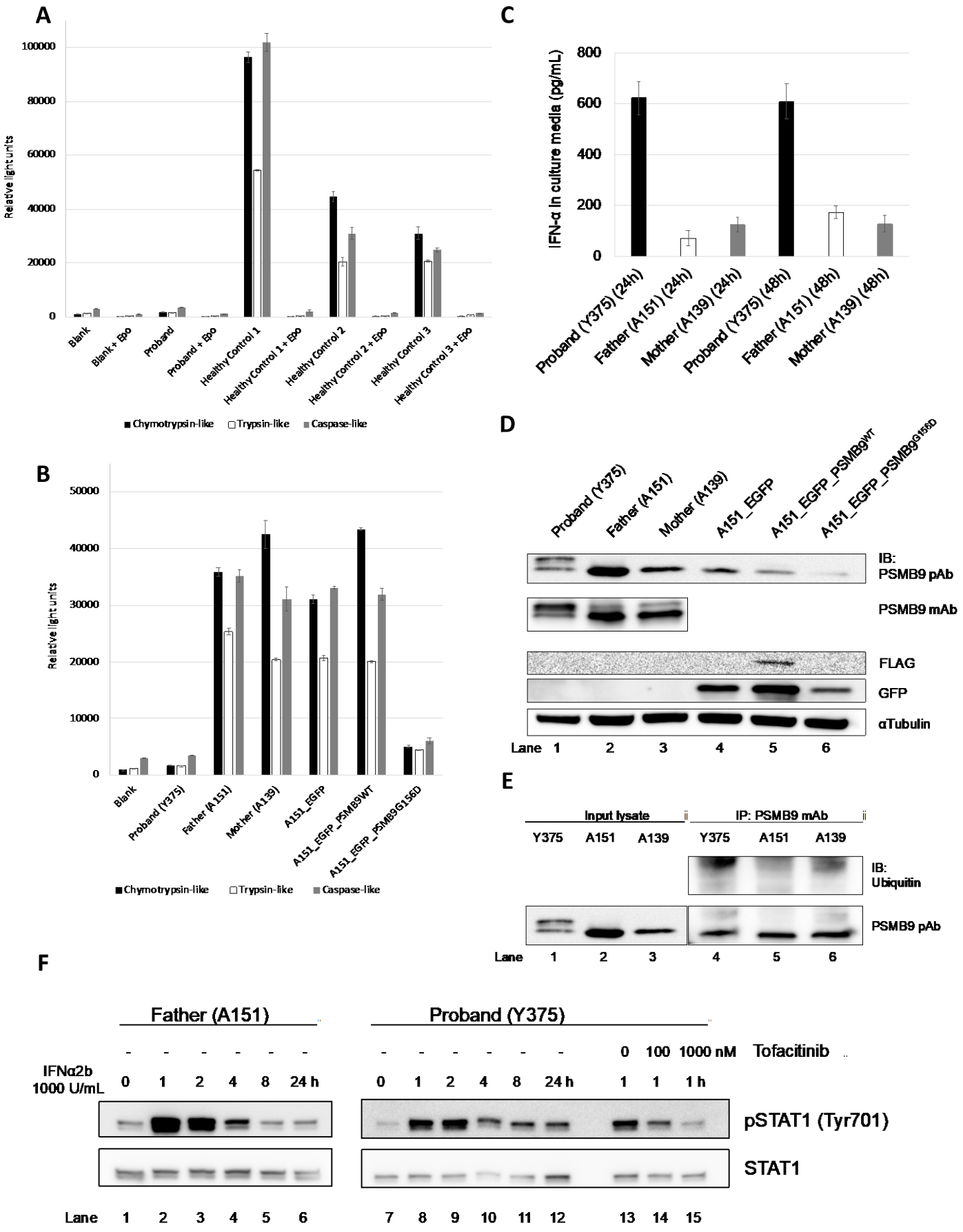
A
Relative light units
100000
80000
60000
40000
20000
0
Blank
Blank + Epo
Proband
Proband + Epo
Healthy Control 1
Healthy Control 1 + Epo
Healthy Control 2
Healthy Control 2 + Epo
Healthy Control 3
Healthy Control 3 + Epo
Chymotrypsin-like
Trypsin-like
Caspase-like
C
IFN-α in culture media (pg/mL)
800
600
400
200
0
Proband (Y375) (24h)
Father (A151) (24h)
Mother (A139) (24h)
Proband (Y375) (48h)
Father (A151) (48h)
Mother (A139) (48h)
B
Relative light units
50000
40000
30000
20000
10000
0
Blank
Proband (Y375)
Father (A151)
Mother (A139)
A151_EGFP
A151_EGFP_PSMB9WT
A151_EGFP_PSMB9G156D
Chymotrypsin-like
Trypsin-like
Caspase-like
D
Proband (Y375)
Father (A151)
Mother (A139)
A151_EGFP
A151_EGFP_PSMB9WT
A151_EGFP_PSMB9G156D
IB: PSMB9 pAb
PSMB9 mAb
FLAG
GFP
αTubulin
Lane 1 2 3 4 5 6
E
Input lysate
IP: PSMB9 mAb
Y375 A151 A139 Y375 A151 A139
IB: Ubiquitin
PSMB9 pAb
Lane 1 2 3 4 5 6
F
Father (A151)
Proband (Y375)
0 100 1000 nM Tofacitinib
IFNα2b 1000 U/mL
0 1 2 4 8 24 h
0 1 2 4 8 24 h
1 1 1 h
pSTAT1 (Tyr701)
STAT1
Lane 1 2 3 4 5 6 7 8 9 10 11 12 13 14 15

Supplemental Information

Methods

Genomic sequencing

We extracted genomic DNA from peripheral blood cells using the QIAamp DNA Blood Mini Kit (QIAGEN, Hilden, Germany). Genomic DNA was captured using SureSelect Human All Exon 50M, V5 Kits (Agilent Technologies, Santa Clara, CA) and analyzed by massive parallel sequencing using a Hiseq 2500 (Illumina, San Diego, CA) next-generation sequencer with a 100 × 2 paired-end option. Candidate germline mutations were detected using a pipeline for whole exome sequencing (WES; Genomon: http://genomon.hgc.jp/exome/) as previously described[1]. For Sanger sequencing of *PSMB9* exon 5, the following primers were used for PCR amplification: forward 5'-GCTGCTGCAAATGTGGTGAG-3' and reverse 5'-AGCAATAGCGTCTGTGGTGA-3'. Written informed consent was obtained from patient's guardians. This study was approved by the ethics committee of the Nagoya University Graduate School of Medicine and was conducted in accordance with the principles of the Declaration of Helsinki.

Structural modeling

Homology modeling for mutant PSMB9 was generated with the human immunoproteasome (PDB entry code: 6AVO) as a template using the UCSF chimera interface to MODELLER[2,3]. The close-up views shows the junction surfaces of 3 combinations of wild-type PSMB9 and mutant PSMB9 proteins.

Cell lines

B lymphoblastoid cell lines (LCL) were established from the proband diagnosed with type I interferonopathy

(Y375) as well as from his father (A151), mother (A139), and three unrelated healthy controls. Y375 harbored a heterozygous missense mutation in *PSMB9* (NM_002800.5: c.467G>A, p.G156D), whereas A151 and A139 had homozygous wildtype (WT) alleles of *PSMB9*.

Lentivirus transduction of PSMB9 in cells

WT and mutant *PSMB9* cDNAs were generated using artificial gene synthesis. Lentiviral packaging constructs, pCAG-HIVgp and pCMV-VSV-G-RSV-Rev, and a cDNA-expressing backbone construct, CSII-CMV-MCS-IRES2-Venus were gifts from Dr. Hiroyuki Miyoshi, RIKEN[4]. Backbone constructs were modified to co-express enhanced green fluorescent protein (EGFP) and blasticidin-S-deaminase (Bsd) under internal ribosomal entry site (IRES)-mediated bicistronic expression to facilitate selection (CSII-CMV-IRES2-EGFP-T2A-Bsd). FLAG-tagged *PSMB9* WT or mutant cDNAs were cloned into the backbone and lentivirus-containing culture supernatants were prepared. For the stable overexpression, A151 cells (i.e., LCLs derived from the proband's father) were cultured, and selected with medium containing blasticidin added to a concentration of 10 μg/mL at 48 h after transfection.

Immunoblot and immunoprecipitation assays

An immunoblot (IB) assay was performed with total cell extracts that were separated on 4%–20% gradient TGX™ gel and transferred on a 0.45-μm nitrocellulose membrane (BioRad, Hercules, CA, USA). Antibodies used included anti-α-tubulin (DM1A, Sigma, St. Louis, MO, USA), anti-FLAG (M2, Sigma), anti-GFP (D5.1 XP, Cell Signaling Technology, Danvers, MA, USA), polyclonal anti-PSMB9 (ab3328, Abcam, Cambridge,

UK), anti-ubiquitin (ab134953, Abcam), anti-PSMB8 rabbit monoclonal antibodies (ab180606, Abcam, UK), anti-PSMB10 rabbit monoclonal antibodies (ab183506, Abcam), anti-Phospho-STAT1 (Tyr701) (58D6) rabbit monoclonal antibodies (#9167, Cell Signaling Technology, Danvers, USA), and anti-STAT1 rabbit monoclonal antibodies (D1K9Y) (#14994, Cell Signaling Technology).

The immunoprecipitation (IP) assay was performed with cells that were lysed in ice-cold IP Lysis Buffer (Thermo Fisher Scientific, Waltham, MA, USA); lysates containing 500 μg of total protein were prepared. Antibodies (1 μg) were bound to Dynabeads™ Protein G (Thermo Fisher Scientific) for 10 min at room temperature; antibody-bound beads were incubated overnight with cell lysates at 4°C. The eluted samples were separated on 4%–20% gradient TGX™ gel and transferred to an Immun-Blot polyvinylidene fluoride (PVDF) membrane (BioRad). The antibodies used for IP included anti-FLAG (M2, Sigma) and monoclonal anti-PSMB9 (ab184172, Abcam). For IB of the IP samples, Clean-Blot™ IP Detection reagent (Thermo Fisher Scientific) was used as a secondary antibody.

Proteasome activity assay

Frozen cell lines were thawed in a water bath at 37°C and resuspended in 10% fetal bovine serum containing Roswell Park Memorial Institute (RPMI) 1640 medium. Cells were counted and 10^4 cells were distributed in each well. Proteasome activities were measured using the Proteasome-Glo™ cell-based assay kit (Promega, Madison, WI) according to the manufacturer's instructions. Briefly, luminescence was recorded using POWERSCAN 4 plate luminometer (DS Pharma Biomedical, Osaka, Japan) to detect the digestion of specific luminogenic proteasome substrates including Suc-LLVY-aminoluciferin (succinyl-leucine-leucine-valine-

tyrosine-aminoluciferin), Z-LRR-aminoluciferin (Z-leucine-arginine-arginine-aminoluciferin), and Z-nLPnLD-aminoluciferin (Z-norleucine-proline-norleucine-aspartate-aminoluciferin) to detect chymotrypsin-like, trypsin-like, and caspase-like activities, respectively. The proteasome inhibitor, epoxomicin, was added at a concentration of 9 μmol/L 2 h prior to the measurement of proteasome activities. All experiments were performed in triplicates; the results shown are the average values.

Enzyme-Linked Immunosorbent Assay (ELISA) to quantify IFN-α

Cells (5×10^5/mL) were cultured in fresh RPMI 1640 media supplemented with 10% fetal bovine serum for the indicated incubation time periods. Then, IFN-α in the cell culture media were quantified using the VeriKine Human Interferon Alpha Multi-Subtype Serum ELISA Kit (41110-1, PBL Assay Science, Piscataway, USA), according to the manufacturer's instructions.

Cell culture with IFNα2b and JAK inhibitor

Cells (5×10^5/mL) were maintained in RPMI 1640 supplemented with 10% fetal bovine serum and subsequently cultured for the indicated time period with IFNα2b (HZ-1072, Proteintech, Tokyo, Japan) 1000 U/mL. The cells were pretreated with 100 or 1000 nM concentrations of Tofacitinib citrate (PZ0017, Sigma-Aldrich Japan, Tokyo, Japan) 30 min before stimulation with IFNα2b for a 1-h-period.

Supplemental References

1. Muramatsu H, Okuno Y, Yoshida K, Shiraishi Y, Doisaki S, Narita A, et al. Clinical utility of next-generation sequencing for inherited bone marrow failure syndromes. Genet Med. 2017;19:796–802.

2. Pettersen EF, Goddard TD, Huang CC, Couch GS, Greenblatt DM, Meng EC, et al. UCSF Chimera─a visualization system for exploratory research and anal- ysis. J Comput Chem 2004;25:1605-12.

3. Webb B, Sali A. Comparative protein structure modeling using MODELLER. Curr. Protoc. Bioinformatics. 2014;47:5.6.1–32.

4. Miyoshi H, Blomer U, Takahashi M, Gage F H, Verma I M. Development of a self-inactivating lentivirus vector. J Virol. 1998;72:8150–8157.

Supplemental Figures

Figure E1. Immunoblot for the subunits of 20S immunoproteasome other than PSMB9 [β5i (PSMB8), β2i (PSMB10)]

Immunoblotting probed with monoclonal anti-PSMB8 and anti-PSMB10 antibodies.

Figure E2. Immunoblots for Phospho-STAT1

Immunoblotting probed with anti-phosphorylated STAT1 (Tyr 701) and anti-STAT1 antibodies.

FIG E1

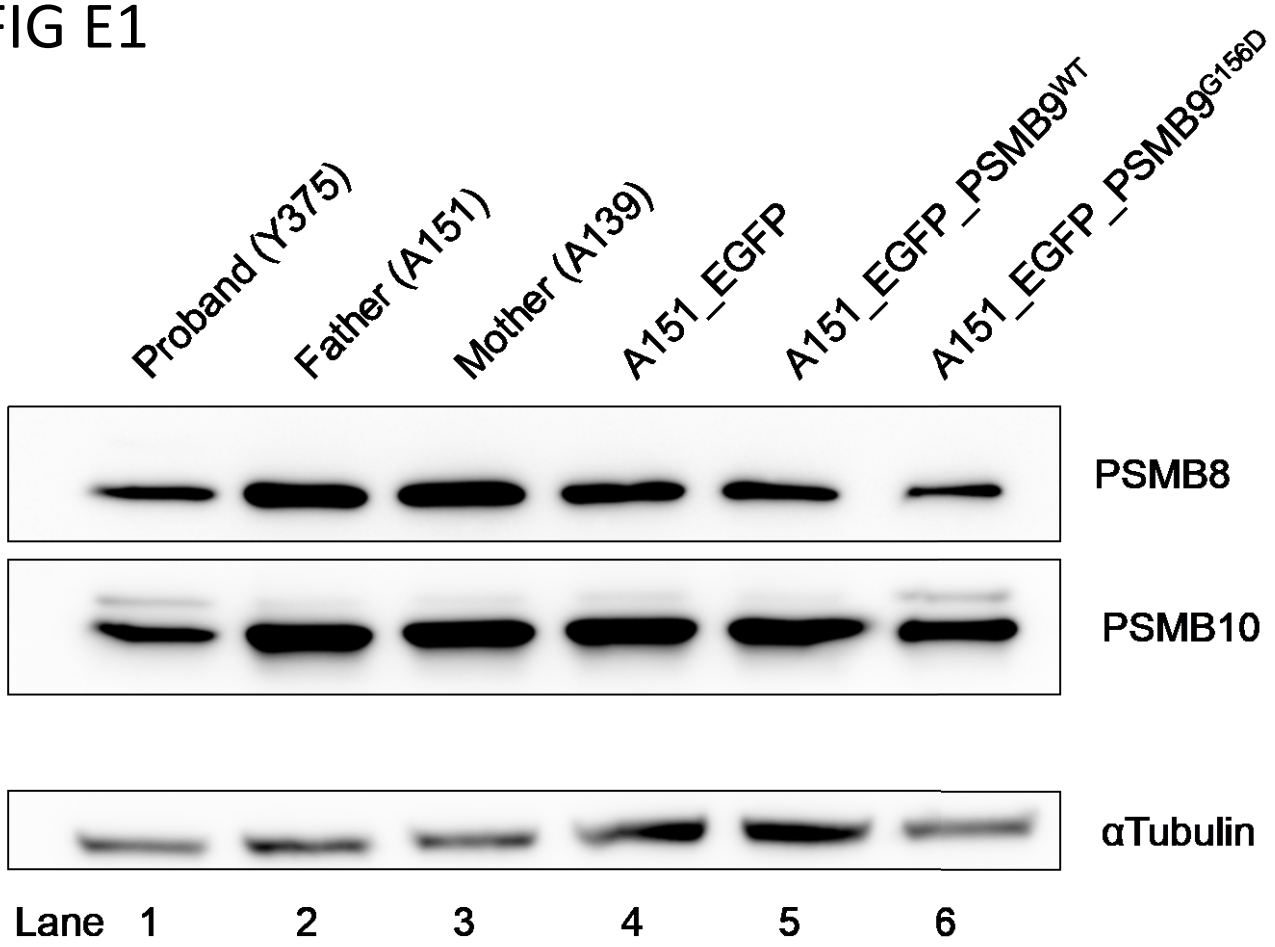
Proband (Y375)
Father (A151)
Mother (A139)
A151_EGFP
A151_EGFP _PSMB9WT
A151_EGFP _PSMB9G156D
PSMB8
PSMB10
αTubulin
Lane 1 2 3 4 5 6

FIG E2

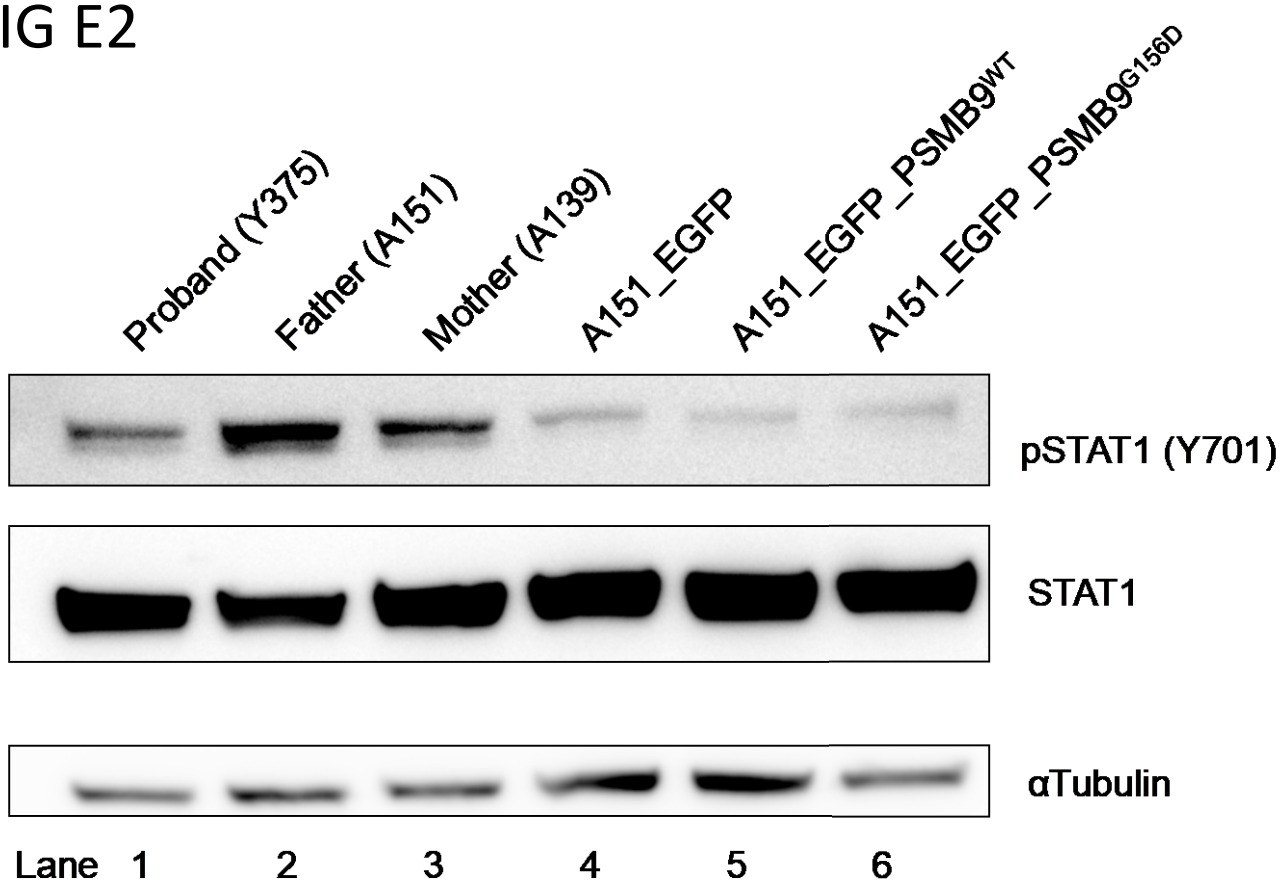
Proband (Y375)
Father (A151)
Mother (A139)
A151_EGFP
A151_EGFP_PSMB9WT
A151_EGFP_PSMB9G156D
pSTAT1 (Y701)
STAT1
αTubulin
Lane 1 2 3 4 5 6

Supplemental Tables

Table E1. Summary of the patient's laboratory values

Blood chemistry		**Standard values for a 1-month-old boy**
Aspartate aminotransferase (U/L)	923	21–64
Alanine aminotransferase (U/L)	426	12–50
Lactate dehydrogenase (U/L)	3165	201–405
Total bilirubin (mg/dL)	0.6	0.3–2.3
Total protein (g/dL)	5.2	4.9–6.6
Albumin (g/dL)	2.8	3.1–4.3
Blood urea nitrogen (mg/dL)	11.5	2.8–14.5
Creatinine (mg/dL)	0.14	0.1–0.6
Creatine phosphokinase (U/L)	26839	44–315
Sodium (mEq/L)	132	135–143
Potassium (mEq/L)	5.3	4.2–5.9
Chloride (mEq/L)	95	101–111
Calcium (mg/dL)	11	9.0–11.0
C-reactive protein (mg/dL)	10.88	0.0–0.3
IgG (mg/dL)	506	166–547
IgA (mg/dL)	12	6–47

IgM (mg/dL)	54	18–98
Myoglobin (ng/mL)	1337	17–106
Troponin T (ng/mL)	0.229	<0.05
Ferritin (ng/mL)	4395	<400

Hematology

White blood cell ($\times 10^9$/L)	3.83	4.7–18.6
Lymphocyte ($\times 10^9$/L)	1.226	4.0–7.0
$CD3^+$ ($\times 10^9$/L)	0.635	3.2–5.4
$CD4^+$ ($\times 10^9$/L)	0.564	2.3–3.6
$CD8^+$ ($\times 10^9$/L)	0.078	0.7–1.4
$CD19^+$ ($\times 10^9$/L)	0.161	0.3–1.4
$CD16^+/56^+$ ($\times 10^9$/L)	0.015	0.2–0.9
Hemoglobin (g/dL)	7.6	9.0–13.5
Platelet ($\times 10^9$/L)	52	27.0–88.0

Coagulation functions

Prothrombin time international normalized ratio	1.4	0.8–1.2
Activated partial thromboplastic time (sec)	38.1	25–40
Fibrinogen (mg/dL)	105	230–450

Fibrin/fibrinogen degradation products (μg/mL)	29.8	<10
D-dimer (μg/mL)	21	<0.5
Antithrombin (%)	33	48–125

Immunological tests

PHA (cpm/S.I.)	111,424/65.3	20,500–56,800
ConA (cpm/S.I.)	64,392/37.7	20,300–65,700

Supplemental Videos

Video E1 and E2: echocardiogram documenting pulmonary hypertension

(E1) Four chamber view using color Doppler before the induction of tofacitinib and veno-arterial extracorporeal membranous oxygenation (VA-ECMO). (E2) Short-axis view before the induction of tofacitinib and VA-ECMO at left ventricular end-diastole.